Indian Journal of Pure & Applied Physics
Vol. 55, March 2017, pp. 231-236

Optoelectronic and antimicrobial activity of composite zinc oxide and cadmium sulphide quantum dots and application in water treatment

J Barman[a]* & Farhana Sultana[b]

[a]Department of Physics, ADP College, Nagaon 782 002, India
[b]Biotech Hub, ADP College, Nagaon 782 002, India

Received 26 March 2016; revised 16 November 2016; accepted 3 January 2017

In the present study, we report the synthesis of composite zinc oxide and cadmium sulphide nanoparticles by a chemical route. ZnO–CdS nanocomposites have been gaining much importance as they show fascinating opto-electronic properties such as tunable band gap and the nanomaterials are suitable for fast photon absorption, transportation and collection. The prepared composite nanoparticles have been characterized by UV–VIS absorption, X-ray diffraction (XRD) and TEM, AFM and FTIR observation. UV-VIS optical spectroscopy study has been carried out to determine the band gap of the composite zinc oxide and cadmium sulphide thin film and it shows a blue shift with respect to the bulk value. The nanocomposites show enhanced optio -electronic properties compared to the individual constituents. The band gap of CdS–ZnO nanocomposites depend on various experimental parameters such as reaction time, concentrations of cadmium salt, and also chemical nature of the cadmium salt. The band gap value of the ZnO–CdS nanocrystalline films are obtained in the range of 3.88–4.14 eV which is higher than that of bulk value of ZnO (3.3 eV) and CdS (2.42 eV). The synthesized nanoparticles exhibited high antibacterial activity and can be used for water purification.

Keywords: Composite, XRD, UV–VIS absorption, Antibacterial

1 Introduction

Zinc oxide and cadmium sulphide nanoparticles have received much attention due to their implications in water treatment and opto-electronic properties[1]. Zinc oxide–cadmium sulfide nanocomposites have been extensively studied due to their applications in the area of optics, electronics and photo catalysis[2-5]. ZnO–CdS core–shell nanostructures have interesting applications in chemical engineering and biology[6–11]. ZnO is technologically an important material for its wide range of optical and electrical properties; also it is a semiconductor crystal with a large binding energy (60 meV) and wide band gap (3.3 eV at 300 K). Such properties make semiconducting nanostructures suitable for several kinds of applications, from anti-reflecting coatings[12] to bioelectronics[13] and light emitting devices[14] antibacterial treatment[15], UV light emitters[16], photocatalyst[17] and as an additive in many industrial products. It is also used in the fabrication of solar cells[15], gas sensors[15], luminescent materials[18], transparent conductor. Inorganic Nanoparticles are important materials for applications in medicine, such as biosensing, cell imaging, drug delivery, cancer therapy etc[17-18]. According to the Project on Emerging Nanotechnologies (PEN), ZnO occupies fifth rank among the most prevalent nanomaterials in consumer products[14]. ZnO can have two different crystal structures (zinc blende and wurtzite), both of which have the same band gap energy (3.3 eV) and the direct band structure. Localized trap states inside the band gap were studied[15] in detail to recognize the sub-band gap energy levels. It was found that the defect levels play an important role in determining the luminescence characteristics of the ZnO and CdS nanoparticles[19.] In the ZnO–CdS nanocomposites, CdS acts as a visible sensitizer while ZnO, a semiconductor with a wide band gap (3.34 eV at 2 K), is responsible for charge separation which suppresses the recombination process[20]. One dimensional ZnO–CdS nanocomposites exhibit attractive optoelectronic properties such as tunable band gap, and the nanostructures are suitable for fast photon absorption, transportation, and collection[21] ZnO–CdS nanocomposites also possess better physicochemical properties compared to the constituents such as enhanced conductivity improved sensing capabilities compared to pure ZnO and CdS[22].

In developing countries, 80% of the diseases are due to bacterial contamination of drinking water. The removal or inactivation of pathogenic microorganisms

*Corresponding author (E-mail: jayantabarman2006@gmail.com)

is most important in wastewater treatment[18]. According to the World Health Organization[17] any water intended for drinking should contain fecal and total coliform counts of 0, in any 100 mL sample. Another serious issue in water resources planning is the protection of water treatment systems against potential chemical and biological terrorist acts[18-19].

Application of nanotechnology which results in improved water treatment options might help us in removing the finest contaminants from water and with induced specificity to a certain pollutant that destroy or immobilize toxic compounds and pathogens. Heterogeneous photocatalysis is currently being considered as a promising technique for water purification in comparison to other conventional methods[23-24]. Nanomaterials have been gaining increasing interest in the area of environmental remediation mainly due to their enhanced surface and also other specific changes in their physical, chemical and biological properties that develop due to size effects. Nanotechnology offers lot of promise in the area of water purification owing to large surface to volume ratios offered by nanostructures[25] and the possibility of preparing photocatalytic membranes by growing semiconducting nanostructures on conventional membranes[26,27]. Research is underway to use advance nanotechnology for purification of drinking water.

2 Experimental Details

2.1 Preparation of nanoparticles

All the chemicals were of analytical grade and purchased from Merck (India). All the chemicals were used as received without further purification. Deionized water was used as a solvent. Different sized ZnO and CdS nanocomposites were prepared by chemical route at room temperature[15]. Aromatic solids like PVA, being good solute to multiple phase system and it provides uniform gaps that are very close to each other and distributes in the form of array. 5 wt% solution of PVA and 2 wt% $CdCl_2$ was mixed. $ZnSO_4$ was added to it in various concentrations (1, 2, 3, 4 wt %) under a high stirring rate (200 rpm) condition under vacuum condition. The constant temperature 70 °C for 3 h was maintained during the process of stirring. The sample under preparation was kept for 12 h for complete dissolution to get a transparent solution. To this solution, 2 wt% Na_2S was added until the whole solution turns into yellow color and concentrated nitric acid was added to the solution to change the pH of the whole solution. The obtained precipitate was then filtered washed and dried at room temperature. After drying, the precipitate was crushed to fine powder with the help of mortar and pestle. The size of the quantum dots formed depends on the number of cadmium ions and zinc ion exchanged.

2.2 Test for conductivity of water

The conductivity of water was tested for three water samples – distilled water, tap water and sewage water using soil and water analyzing kit.

2.3 Test for antibacterial activity

Escherichia coli (MTCC 739), Klebsiella pneumonia (MTCC 432), Staphylococcus aureus (MTCC 96) and Bacillus subtilis (MTCC 441) were used for antibacterial screening. The microbial cultures were purchased from the "Microbial Type Culture Collection and Gene Bank" (MTCC), Chandigarh, India. The bacterial cultures were maintained on nutrient agar slants and were stored at -4 °C.

2.3.1 Antibacterial assay

Antibacterial assay of composite ZnO and CdS nanoparticles were studied by Well Diffusion Method[28]. The nutrient agar plates were inoculated with 2.0 mL of inoculum by spreading the swab over the plate. The plates were then allowed to dry for 15 min. With the help of sterile borer, wells of 8 mm diameter were cut on the agar plates and loaded with composite ZnO and CdS nanoparticles dissolved in DMSO at desired concentration and a standard antibiotic Tetracyclin as positive control. All plates were incubated at 37 °C for 24 h. After incubation period, the inhibition diameters were measured with Hi-Media scale[29-30]. The data were analyzed using origin graphic software and SPSS software.

3 Results and Discussion

3.1 X-ray diffraction analysis

Figure 1 shows XRD patterns of polymer-capped composite ZnO and CdS nanocrystalline films deposited on glass substrate for different mixing ratio. The XRD pattern contain broad peaks at $2\theta = 26.6°$ at the composite ratio of ZnO: CdS =2:5, $2\theta = 28.06°$ at the ratio of ZnO: CdS =3:5 and $2\theta = 30.06°$ at the ratio ZnO: CdS =4:5 indicating the formation of nanostructure. The peak observed near $2\theta = 19.5°$ is due to the crystalline phase of PVA with a shallow shoulder corresponding to the amorphous part of the polymer. Some individual peaks of ZnO and CdS are also observed. The diffraction peaks at angles near $2\theta = 28.99°$ and $2\theta = 48.15°$ corresponds to (111) and (220) planes of the cubic zincblende (Z) phase of

ZnO. X-ray peak intensities are weak and broad compared to bulk counterpart suggesting small crystallite size. The X-ray peaks are also found to shift to higher diffraction angle with increasing mixing ratio indicating lattice contraction. The lattice contraction is expected to occur because of higher surface to volume ratio with decreasing crystallite size and increase in strain. The shifting of peak position to higher diffraction angle due to strain was confirmed by calibrating the XRD prior to each observation using standard silicon sample. The XRD patterns of prepared sample were taken at operating at 40 kV-30 mA. The radiation source used was Cu K_α (λ =1.542Å) and a Nickel filter was used to block K_β radiations.

Some separate peaks are also observed which may be due to CdO because XRD patterns were recorded in ambient condition. The change of phase from hexagonal wurtzite to cubic is observed in nanocrystallite as compared to their bulk counterpart. The grain size of the crystallite is estimated by Scherer formula[4]:

$$D_{hkl} = K\lambda/w\cos\theta \quad \ldots (1)$$

w being FWHM and θ is the Braggs angle and K= 0.89 for spherical shape (from HRTEM). For calculation w is observed by zooming the peak position using origin graphics software. The calculated size is found between 4.07-7.09 nm.

3.2 Characterization of composite zinc oxide and cadmium sulphide nanoparticles using UV-Vis spectra analysis

The optical absorption of samples is shown in Fig. 2. The UV-Vis spectrophotometer (Systronics 119) and the absorption spectra were recorded at room temperature over the range 300 nm to 800 nm. The observed blue shift in the absorption edge is indication of band gap increase owing to quantum confinement effect.

The fundamental absorption, which corresponds to electron excitation from the valence band to conduction band, can be used to determine the nature and value of the optical band gap. The relation between the absorption coefficient (α) and the incident photon energy ($h\upsilon$) can be written as:

$$(\alpha h\upsilon)^{1/n} = A\,(h\upsilon - E_g) \quad \ldots (2)$$

where A is a constant and Eg is the band gap of the material and exponent n depends on the type of transition. For direct allowed transition n = 1/2 and for indirect allowed transition n = 2. To determine the possible transition, $(\alpha h\upsilon)^2$ versus $h\upsilon$ were plotted (Fig. 3) and

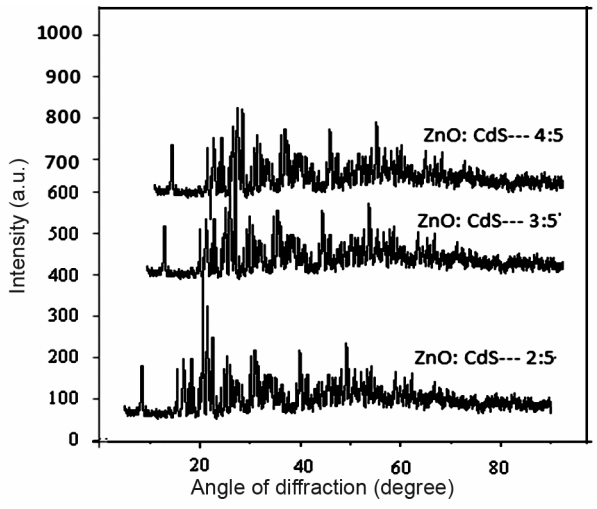

Fig. 1 – XRD patterns of ZnO–CdS nanocomposites prepared using different ratios, ZnO: CdS at 2:5 and 3:5 and 4:5

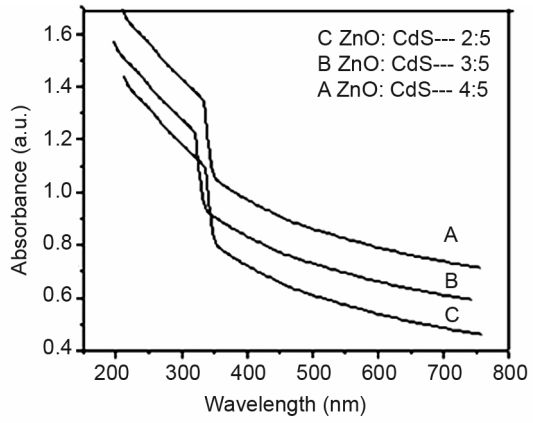

Fig. 2 – Optical absorption of different composite ratio of ZnO and CdS

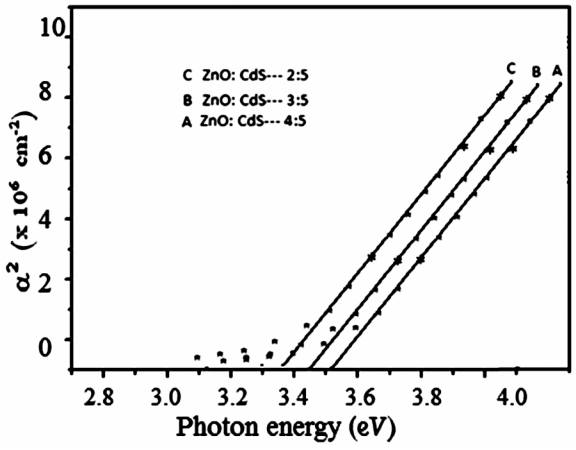

Fig. 3 – Band gap of different composite ratio of ZnO and CdS

corresponding band gaps were obtained by extrapolating the straight line portion of the curves to $(\alpha h\upsilon)^2 = 0$. The band gap values thus obtained are in the range of 3.88–4.14 eV. The direct band gap value of the nanocrystalline films are found to be higher than that of bulk value of ZnO (3.3 eV) and CdS (2.42 eV). The absorption spectra also reveal that the excitonic absorption peaks for all these samples are blue shifted compared to the bulk, indicating strong confinement. Size quantization of carriers in a small volume crystallite is well-known to cause the blue shift. The shift of band gap can be utilized in determining the crystal radius (r) using the effective mass approximation relation:

$$E_{gn} = [E^2_{gb} + 2\hbar^2 E_{gb}(\pi/R)^2 / m^*]^{1/2} \quad \ldots (3)$$

where, m^* is the effective mass of the specimen, E_{gb} is bulk band gap of average value of ZnO and CdS and E_{gn} is the calculated band gap energy. The corresponding particle size is 7 nm for A, 5.5 nm for B and 5.98 nm for C, which is in good agreement determined by XRD and HRTEM observation. It is observed that with increase of composing ratio of ZnO and CdS the band gap increases and particle size decreases. Figure 4 shows the optimum range of composite synthesis ratio.

It is clear from the Table 1 that the direct band gap increases with increase of composite ratio and the particle size increases with increase of pH. In acidic condition OH^- acts as a catalyst for growing ZnO nanoparticle. OH^- may increase the ionization strength of Zn^{2+} for the faster reaction with O in order to accelerate the growth of ZnO nuclei. As the number of nuclei increases, smaller particle coalescence and bigger particles are produced, where the exchange reaction between the O of ZnS and OH^- may have slowed down compared to the exchange reaction which occurred in higher pH.

3.3 TEM and AFM observation

For direct imaging of nanoparticle and their actual distribution, HRTEM observations were taken at a very high magnification. Prior to HRTEM observation polymer-capped mix ZnO and CdS films were deposited on carbon-coated Cu grids. Figure 5 shows HRTEM

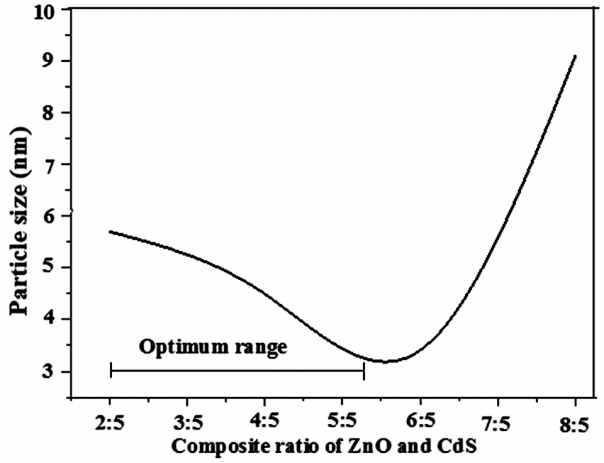

Fig. 4 – Optimum composite ratio of ZnO and CdS

Table 1 – The direct band gap from absorption data and particle size from HBM models

Sample	Composite ratio	Direct band gap of nano structured ZnO (eV)	Direct band gap of nano structured CdS (eV)	Composite band gap (eV)	Particle size from HBM model
A	2:5	3.63	2.65	3.36	4.8
B	3:5	3.71	2.79	3.45	4.87
C	4:5	3.83	3.06	3.54	4.97

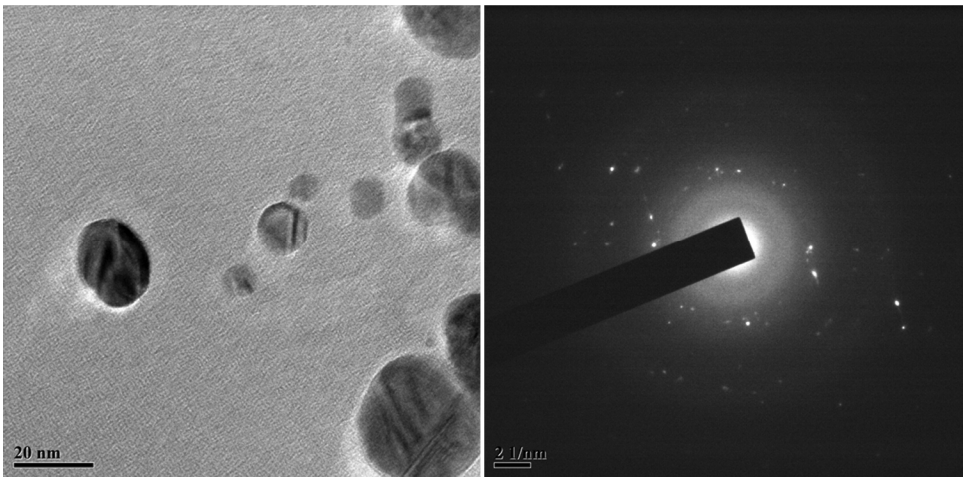

Fig. 5 – HRTEM image of composite Zinc oxide and Cadmium sulphide nanoparticles

micrographs of capped nanocrystalline composite ZnO and CdS in thin films form. The micrograph shows the formation of nearly spherical crystallites having diameter in the range of 7–8 nm for different mixing ratio. The average particle sizes obtained from HRTEM observations were found to be nearly similar as those obtained from XRD and HBM model.

Figure 6 shows the EDX pattern of composite ratio of ZnO and CdS. SEM observation is not shown here. The pattern shows the content of Zn, Cd and Si and O. Si may be arises from glass substrate and O arises because samples were taken in ambient condition.

Figure 7 shows the 3D view of another sample at ZnO: CdS = 4:5 of scan area 2000 nm×2000 nm. Both the pictures indicate that the ratio controls the surface roughness and particle size and its distribution.

3.4 Change in conductivity of water after adding ZnO nanoparticles

Change in conductivity of three different water samples were shown in the Table 2. There is an increase in conductivity of water was observed after adding nanopareticles.

3.5 Antibacterial activity

Antibacterial activity of the synthesized composite zinc oxide and cadmium sulphide nanoparticles was studied for four pathogenic bacteria species. The antibacterial activity was determined *in-vitro* by measuring zone of inhibition in mm using samples at different concentration. Tetracyclin of 1 mg/mL, concentration was used as a control antibacterial agent. The synthesized nanocomposites diffuse in the agar medium and inhibit the growth of the microbial strain tested. The results shown in the Table 3 depict that mix Zinc oxide and Cadmium sulphide nanoparticles are efficiently giving zone of inhibition. NPs penetrate the bacterial cells through holes, pits or protrusions of cell wall. There are different probable mechanisms to explain antibacterial activity of nanoparticles like metal ions uptake into cells, intracellular depletion and disruption of DNA replication, releasing metallic ions and ROS generation etc. Adhesion of released of metallic ions on the cell membrane cause mechanical damage to the cell wall[31].

4 Results and Discussion

Our study was focused on chemical route synthesis of ZnO and CdS nanoparticles. The results from UV-VIS spectroscopy and XRD analysis confirms the synthesis of nano sized mix ZnO and CdS which was then used for water conductivity testing and

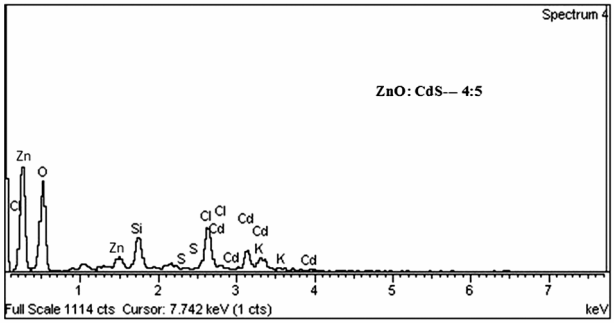

Fig. 6 – EDX pattern of different composite ratios of ZnO and CdS

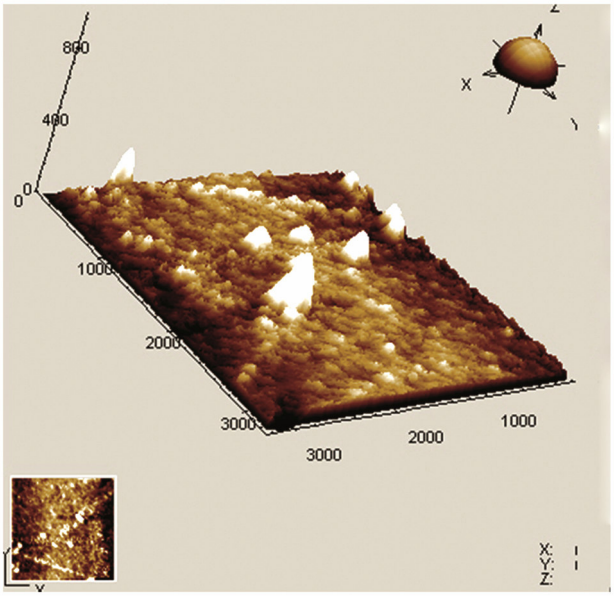

Fig. 7 – AFM image of composite ratio of ZnO and CdS

Table 2 – change in conductivity of water samples before and after adding ZnO nanoparticles

Water sample	Change in conductivity	
	Before adding ZnO and CdS nanoparticles	After adding ZnO and CdS nanoparticles
Distilled water	13.34 µs/cm	2.08 ms/cm
Tap water	0.716 ms/cm	2.69 ms/cm
Sewage water	0.415 ms/cm	2.23 ms/cm

Table 3 – Antibacterial efficacy of ZnO nanoparticles and standard antibiotic against four bacterial strains

Bacterial Strains	Zone of inhibition of mix ZnO and CdS nanopareticles (mm)			Tetracyclin (1 mg.mL^{-1})
	50 µg/L	80 µg/L	100 µg/L	
E. coli	18±0.14	20±0.11	24±0.13	35±0.08
K. pneumonia	19±0.11	21±0.16	26±0.15	32±0.09
B. subtilis	13±0.15	18±0.14	27±0.11	31±0.09
S. aureus	16±0.11	22±0.08	29±0.11	34±0.11

antibacterial assay. The mix ZnO and CdS nanoparticles are effective in increasing the conductivity of water. We also performed antibacterial assay using well-diffusion assay. The large surface area-to-volume ratio allows their use as novel antimicrobial agents. Special focus was given to mechanisms of action which is the most recent issue in the antibacterial activity. The intracellular ROS generated and released metallic ions kill the bacteria. The potential antibacterial action of mix ZnO and CdS nanoparticles has opened up new avenues of antimicrobial applications which are of recent concern for researchers. These nanomaterials also possess unique properties as well as tremendous stability in comparison to organic-based disinfectants.

5 Conclusions

The composite ZnO and CdS nanoparticles were synthesized successfully through chemical route and their structural as well as optical properties were investigated by using UV-VIS spectrophotometer and XRD. The UV -Visible spectra show a large blue shift attributing the enhanced optical properties changes. We also tested for change in conductivity of water after adding mix ZnO and CdS nanoparticles. In case of all the three water samples, we observed an increase in conductivity. The mix ZnO and CdS nanoparticles also showed tremendous antibacterial activity against the water borne pathogens we tested and may be used for water purification. Again mixing ratio takes an important role in outcome result.

Acknowledgement

The author would like to acknowledge UGC for major project and DBT- BIOTECH Hub programme, Department of Biotechnology (DBT), Ministry of Science & Technology and ASTEC, Govt of Assam for financial assistance. We would also like to acknowledge NEHU and USIC, GU for providing us XRD facility.

References

1 Visaria R K, Griffin R J, Williams B W, Ebbini E S, Paciotti G F & Song C W, *Mol Cancer Ther*, 5 (2006) 1014.
2 Panda S K, Chakrabarti S, Satpati B, Satyam P V & Chaudhuri S, *J Phys D: Appl Phys*, 37 (2004) 628.
3 Fang F, Zhao D X, Li B H, Zhang Z Z, Zhang J Y & Shen D Z, *Appl Phys Lett*, 93 (2008) 233115.
4 Vasa P, Taneja P, Ayyub P, Singh B P & Banerjee R, *J Phys Condens Matter*, 14 (2002) 281.
5 Wang X, Liu G, Lu G Q & Cheng H M, *Int J Hydrogen Energy*, 35 (2010) 8199.
6 Meng X Q, Zhao D X, Zhang J Y, Shen D Z, Lu Y M, Fan X W & Wang X H, *Mater Lett*, 61 (2007) 3535.
7 Rajeshwar K, Tacconi N R de & Chenthamarakshan C R, *Chem Mater*, 13 (2001) 2765.
8 Alivisatos A P, *Science*, 271 (1996) 933.
9 Anderson M A, Gorer S, Penner R M, *J Phys Chem B*, 101 (1997) 5895.
10 Caruso F, *Adv Mater*, 13 (2001) 11.
11 Thambidurai M, Muthukumarasamy N, Arul N S, Agilan S, Balasundaraprabhu R, *J Nanoparticles Res*, 13 (2011) 3267.
12 Barman J, Sarma K C, Sarma M & Sarma K, *Indian J Pure Appl Phys*, 46(2008) 339.
13 Bora J P, Barman J & Sarma K C, *Int J Mod Phys*, 24(29) (2010) 5663.
14 Barman J & Sarma K C, *Indian J Phys*, 82(7) (2008) 855.
15 Barman J, *Int J Nanosci Nanotechnol*, 5(2) (2015) 25.
16 World Health Organization, *Guidelines for drinking-water quality*, Geneva WHO, 2(1996).
17 US Environmental Protection Agency, *Alternative disinfectants and oxidants guidance manual*, EPA Office of Water Report 815-R-99-014 (1999).
18 US Environmental Protection Agency, *Variance technology findings for contaminants regulated before 1996*, EPA Opace of Water.Report 815-R-98-003(1998).
19 Baruah S & Dutta J, *Chem Lett*, 7 (2009) 1.
20 J Nayak, S N Sahu, J Kasuya & S Nozaki, *Appl Surf Sci*, 254 (2008) 7215.
21 G J Lee, Y P Lee, H Lim, H Cheong, B H Kil & S H Han, *J Korean Phys Soc*, 58 (2011) 1290.
22 T Gao, Li Q & Wang T, *Chem Mater*, 17 (2005) 887.
23 Sugunan A & Dutta J, *Nanotechnology*, 3 (2008).
24 Hornyak G L, Dutta J, Tibbals H F & Rao A K, *Introduction to nanoscience*, (CRC Press), 2008.
25 Baruah S, Jaisai M, Imani R, Nazhad M M & Dutta J, *Sci Technol Adv Mater*, 11 (2010) 055002.
26 Baruah S, Thanachayanont C & Dutta J, *Sci Technol Adv Mater*, 9 (2008) 025009.
27 Herron N, Wang Y & Eskert H, *J Am Chem Soc*, 112(1990) 1322.
28 Perez C, Paul M & Bazeraue P, *Acta Biol Med Exp*, 15 (1990) 113.
29 Nakamura C V, Nakamura T U, E Bando, Melo A F N, Cortez D A G & Filho B P D, *Mem Inst Oswaldo Cruz*, 94 (1999) 675.
30 Saikia M & Handique P J, *J Med Plant Res*, 7 (2013) 1330.
31 Sirelkhatim A, Mahmud S, Seeni A, Mohamad Kaus N H & Ann L C, *Nano-Micro Lett*,7 (2015) 219.